Direct-Drive Shock-Ignition for the Laser Megajoule.

B. Canaud*, S. Laffite, V. Brandon
CEA, DAM, DIF, F-91297 Arpajon, France

M. Temporal, R. Ramis
ETSIA, Universidad Politecnica de Madrid, Spain

(Dated: October 13, 2011)

We present a review of direct-drive shock ignition studies done as alternative for the Laser Mega-Joule to achieve high thermonuclear gain. One-dimensional analysis of HiPER-like Shock-ignited target designs is presented. It is shown that high gain can be achieved with shock ignition for designs which do not ignite only from the laser compression. Shock ignition is achieved for different targets of the fast ignition family which are driven by an absorbed energy between 100 kJ and 850 kJ and deliver thermonuclear energies between 10-130 MJ. Shock-Ignition of Direct-Drive Double-Shell non-cryogenic target is also addressed. 2D results concerning the LMJ irradiation geometry are presented. Few systematic analyses are performed for the fuel assembly irradiation uniformity using the whole LMJ configuration or a part of the facility, and for the ignitor spike uniformity. Solutions for fuel assembly and shock ignition on LMJ using 2D calculations are presented. It is shown that high-gain shock-ignition is possible with intensity of each quad less than 1e15 W/cm^2 but low modes asymmetries displace the ignitor power in the spike towards higher powers..

PACS numbers: 52.57.Bc, 52.57.-z,52.35.Tc,52.57.Kk

I. INTRODUCTION

Direct drive inertial fusion is an alternative to achieve inertial confinement fusion for the laser Megajoule (LMJ) for a decade [1–7]. This approach is an alternative to the indirect drive [8] to reach high thermonuclear energy and gain. In the direct drive, laser beams overlap on the external side of a spherical target and the irradiation uniformity has to be addressed carefully [9–11] in order to improve target hydrodynamic stability [12, 13]. However, the LMJ beam layout for direct-drive self ignition requires zooming technics [4, 6] and without this technic the target should be only marginally igniting.

Recent works at the University of Rochester [14] proposed a non-isobaric ignition of the fuel, called Shock Ignition, which consists in separating the fuel assembly (at low adiabat and velocity) from the ignition produced by a convergent ignitor shock. This very promising solution was recently proposed to ignite the Fast Ignition capsule of HiPER [15, 16].

We address here the possibility of using this technic for LMJ using HiPER-like target. In a first section, 1D-analysis is used to design a target and a laser pulse in scaled up from the HiPER target. The second section is devoted to 2D-calculations, considering the LMJ beam layout and a third section is devoted to direct-drive shock-ignition of double shell targets [17].

II. 1D-ANALYSIS OF DIRECT-DRIVE SHOCK IGNITION FOR LMJ

In order to obtain a scaled target design for LMJ we scale up [18] the HiPER target as described in FiG.1. We

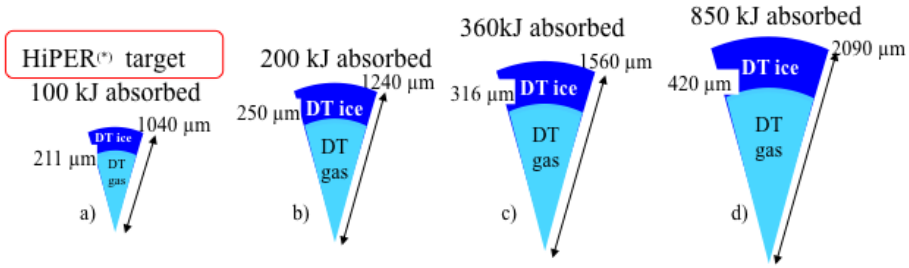

* Corresponding author: benoit.canaud@cea.fr

FIG. 1: different target designs produced by a scaling up of the hiPER target.

then considered the shock ignition of each target done by adding a timed laser spike. Calculations are done with the one-dimensional Lagrangian radiation-hydrodynamics code FCI1[19] usually used for ICF design studies at CEA, DIF. It includes tabulated equations of state (e.g. SESAME), flux-limited Spitzer heat transport (here the flux limiter is set at 6 %), multigroup radiative transfer, one-dimensional ray-tracing, multigroup alpha particle transport, and neutron transport.

The thermonuclear gain obtained for each target and each spike power is given in FIG.2. It is also shown scaling curve (in black, in the left). Figure 2-A shows that each design has an ignitor power threshold above which the gain passes a maximum and decreases after. Below it, the target is not igniting. This power threshold, that is defined as the power corresponding to the maximum gradient of each gain curve of Fig.2-A, decreases when target approaches the isobaric ignition threshold. This is due to the fact that targets closer to the isobaric ignition threshold (curve in black, on FIG.2-B) require lower peak ignitor power.

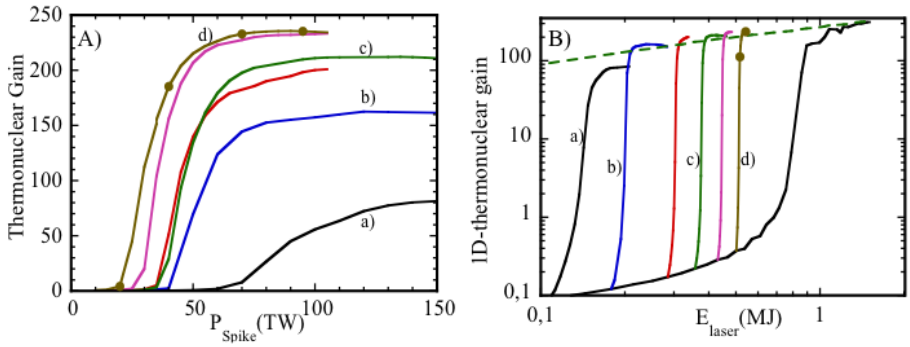

FIG. 2: Shock-Ignition and thermonuclear gain for each HiPER-like designs versus the spike power (A) and the kinetic energy (B).

From this set of target designs we extract one (target c in FIG.1) which seems to match the LMJ energy requirements for fuel assembly and shock ignition.

III. 2D ANALYSIS OF DIRECT-DRIVE SHOCK IGNITION FOR LMJ

The LMJ will be a 240-beamlet frequency-trippled (3ω-0.35 μm) Nd-glass laser facility with a maximum energy and power of 1.8 MJ and 600 TW respectively. Beams are grouped by four in sixty bundles distributed around the target chamber, in 3 rings per hemisphere at the polar angles of 33.2^o, 49^o, and 59.5^o. 10 quads are distributed equally in each ring. Between each ring, quads azimuthal angles are shifted by $\pi/20$ and both hemispheres are shifted also one to the other with the same angle.

In previous works [6, 7], we showed that the fuel assembly of a conventional DD-target could be done with only the rings, at 49^o and 59.5^o, with a total available energy of about 1 MJ. In addition, the ring at the polar angle of 33.2^o is unemployed in this configuration and could be used for shock ignition with a maximum laser power of 200 TW.

The target considered here is the target (c) described in Fig.1. The 1D-laser pulse drives the 1D-implosion on a low in-flight adiabat (defined as the ratio of the multiple-shock induced-pressure over the Fermi pressure : $\alpha = P[TPa]/2.17\rho^{5/3}[kg/m^3] \sim 0.8$) at a peak implosion velocity of 290 km/s. At stagnation, the peak areal density is $\rho r \sim 19$ kg/m^2 and peak density is $\rho \sim 680 \times 10^3$ kg/m^3.

In a first step, we consider 1D-calculation of the fuel assembly with 1D-centered laser beams and an additional laser beam located at a polar angle of 33.2^o in order to create the ignitor shock by a laser spike. In calculations, this last laser beam is modelized by 3D-ray tracing algorithm. The focal shape is top-hat circular intensity profile with a radius r_0 varying from 0.8 to 1.2 mm. The spike is a 300 ps long flat laser pulse with 200 ps rise and fall times. A variation of spike power P_{spike} and pulse timing between driver and spike is performed to find the ignition window. The thermonuclear gain is defined by: $G = E_{th}/(E_{1D}/\eta_{3D} + E_{spike})$ where E_{1D}, $\eta_{3D} \sim 0.5$, and E_{spike} are the 1D-fuel assembly drive energy, the laser-target coupling efficiency η_{3D} in 3 dimensions and the ignitor spike energy respectively. As it can be seen, smaller the focal spot, better the laser-target coupling is, and lower the ignitor spike power has to be. When the ignitor focal spot radius is larger, the ignitor shock is much more isotropic and ignition requires less intensity in the spike to achieve ignition and gain. In addition, the increase of the radius leads to a quadratic reduction of the intensity needed to ignite the target. From Fig.3-b, it can be seen that the intensity in

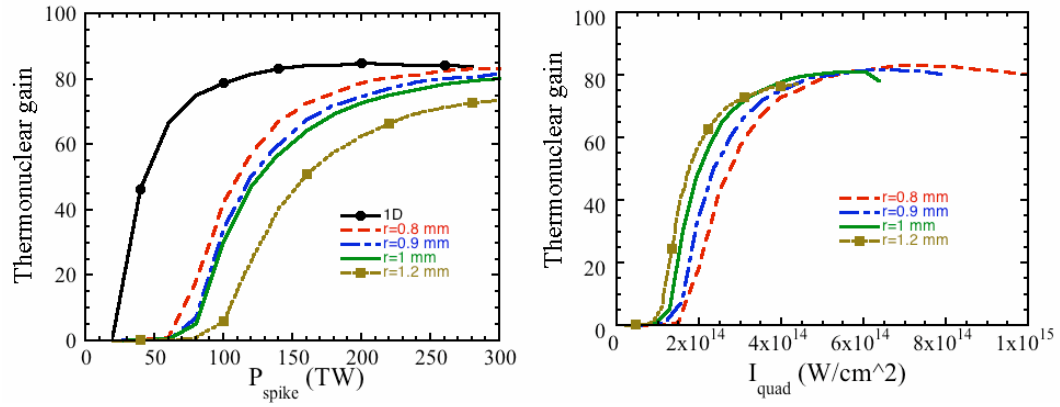

FIG. 3: Thermonuclear gain versus the spike power (a) and spike intensity (b) of each quad for the ring@33.2^o for different focal spot radii (0.8 mm : dashed line, 0.9 mm: dot-dashed-line,1 mm: plain line, and 1.2 mm: dotted line and squares) compared the full-1D calculation (plain line and circles).

each quad is at a low level of few 10^{14} W/cm^2. However, this intensity is superimposed to the fuel assembly intensity which is about 2×10^{14} W/cm^2. Nevertheless, the resulting intensity stays at low level, well below 10^{15} W/cm^2. These results show that to choose a target design not so far from the self-ignition threshold allows to reduce the intensity of the ignitor spike at level of the order of two-plasmon decay threshold.

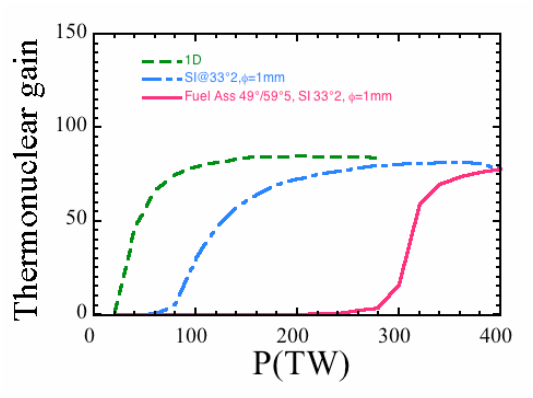

FIG. 4: Thermonuclear gain versus the spike power for full-1D calculation (dashed line), for 1D-full assembly and shock ignition at @33.2^o (dot-dashed line), and for full 2D calculation (2D full assembly and 2D shock ignition, plain line).

We then consider the full 2D problem of fuel assembly and shock ignition by using two rings located at polar angles of 49^o and 59.5^o for fuel assembly and 33.2^o for shock ignition. Calculations used a top-hat intensity profile, a focal spot radius equal to $0.9\times r_{target}= 1.4$ mm, and the same ring-to-ring power balance. The laser pulse is reshaped in comparison to the 1D-pulse in order to take into account the 3D aspect of the laser beams (especially the energy losses by the side of the imploding target). Zooming is not considered here. The irradiation uniformity is not fine but sufficient to ensure a relative good isotropy of the implosion. However, a reduction of the peak density and areal density is observed due to the anisotropy of the stagnating shell. Indeed, the areal density changes from 18.5 kg/m^3 to 16 kg/m^2 with a rms deviation of 37 %. The implosion velocity and the in-flight adiabat are kept similar to the 1D ones.

Shock ignition is done by the use of beams located at polar angle of 33.2^o with a top-hat intensity profile and a radius of 1 mm. A variation of spike time of launch and power is done in order to achieve high thermonuclear gain. Fig.4 shows a comparison of shock ignition for the full-1D calculations, for 1D-full assembly and 2D shock ignition, and for the full 2D calculations. It can be seen that high thermonuclear gain is achieved for higher spike power in full 2D-calculations. This power increase is manly due to strong low mode asymmetries observed at stagnation due to the full assembly done in a quasi-direct drive beam geometry. This beam layout has a strong consequence on self-ignition threshold and displaces it towards higher energies as observed previously in the baseline direct-drive target design[6]. As the self-ignition threshold is at higher level, the power need to reduce it by shock ignition is more important.

IV. SHOCK IGNITION OF DIRECT-DRIVE DOUBLE-SHELL TARGET.

Shock ignition is investigated for non-cryogenic direct-drive double-shell targets [17]. This concept consists in accelerating an external shell (see FIG.5) to high velocity (few hundreds km/s) that goes to impact a high-Z inner shell enclosing DT gas. The fuel assembly is obtained by direct laser light absorbed in the external shell. The ignition is produced by a spherically convergent shock launched by a laser spike added at the end of the main laser drive. A moderate thermonuclear gain (1-10) is obtained for a well-synchronized, high-pressure ignitor shock. The last is

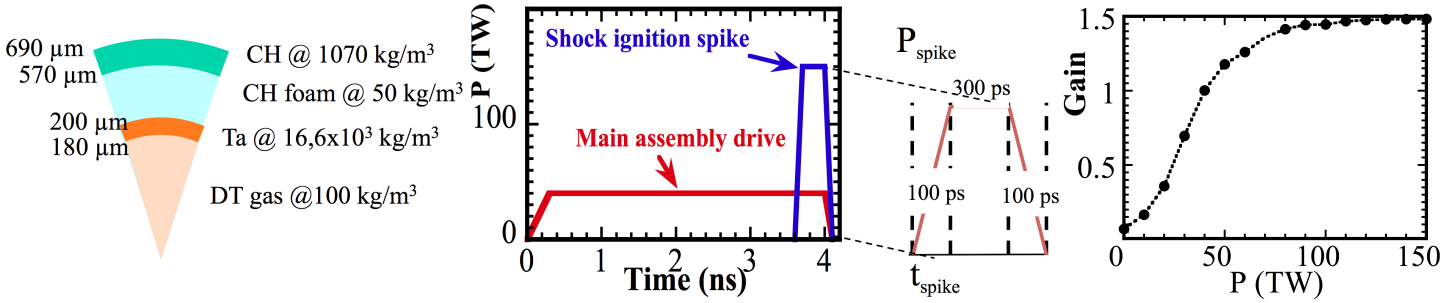

FIG. 5: Shock-Ignited direct-drive double-shell design (laser and target).

produced by a 300 ps-few hundred TW laser spike added at the end of the drive pulse. We have shown also that keeping constant the main drive implies a modification of the peak implosion velocity and leads to a lower ignition spike power threshold than the one needed when the implosion velocity is kept constant by reducing the main drive.

V. CONCLUSIONS.

Direct-drive shock ignition is studied for LMJ for cryogenic HiPER-like target and double shell non-cryogenic target. High gain can be achieved with shock ignition for cryogenic targets. Shock ignition is achieved for different targets of the fast ignition family which are driven by an absorbed energy between 100 kJ and 850 kJ and deliver thermonuclear energies between 10-130 MJ. Moderate gains are achieved for double-shell targets. 2D calculations show that high-gain shock-ignition is possible with intensity of each quad less than 1e15 W/cm2 but low modes asymmetries displace the ignitor spike power towards higher powers.

[1] X. Fortin and B. Canaud, Inertial Fusion Science and Applications (1999).
[2] B. Canaud, X. Fortin, F. Garaude, C. Meyer, F. Philippe, M. Temporal, S. Atzeni, and A. Schiavi, Nucl. Fusion **44**, 1118 (2004).
[3] B. Canaud, X. Fortin, F. Garaude, C. Meyer, and F. Philippe, Las. Part. Beam. **22**, 109 (2004).
[4] B. Canaud and F. Garaude, Nucl. Fusion **45**, L43 (2005).
[5] D. Riz, F. Garaude, M. Houry, and B. Canaud, Nucl. Fusion **46**, 864 (2006).
[6] B. Canaud, F. Garaude, C. Clique, N. Lecler, A. Masson, R. Quach, and J. Van der Vliet, Nucl. Fusion **47**, 1652 (2007).
[7] B. Canaud, F. Garaude, P. Ballereau, J. L. Bourgade, C. Clique, D. Dureau, M. Houry, S. Jaouen, H. Jourdren, N. Lecler, et al., Plasma Phys. Control. Fusion **49**, B601 (2007).
[8] J. Giorla, J. Bastian, C. Bayer, B. Canaud, M. Casanova, F. Chaland, C. Cherfils, C. Clique, E. Dattolo, P. Fremerye, et al., Plasma Phys. Contr. Fusion **48**, B75 (2006).
[9] B. Canaud, X. Fortin, N. Dague, and J. Bocher, Phys. Plasmas. **9**, 4252 (2002).
[10] M. Temporal and B. Canaud, Eur. Phys. J. D **55**, 139 (2009).
[11] M. Temporal, R. Ramis, and B. Canaud, J. phys.: Conf. Series **244**, 022008 (2010).
[12] M. Temporal, S. Jaouen, L. Masse, and B. Canaud, Phys. Plasmas **13**, 122701 (2006).
[13] J. Sanz, J. Garnier, C. Cherfils-Clerouin, B. Canaud, L. Masse, and M. Temporal, Phys. Plasmas **12**, 112702 (2005).
[14] R. Betti, C. Zhou, K. Anderson, L. Perkins, W. Theobald, and A. Solodov, Phys. Rev. Lett. **98**, 155001 (2007).
[15] M. Dunne, Nat. Phys. **2**, 2 (2006).
[16] X. Ribeyre, G. Schurtz, M. Lafon, S. Galera, and S. Weber, Plasma Phys. Control. Fusion **51**, 015013 (2009).
[17] B. Canaud, S. Laffite, and M. Temporal, Nucl. Fusion **51**, 062001 (2011).
[18] E. Falize and C. Michaut and S. Bouquet, Astrophys. J. **730**, 96 (2011).
[19] E. Buresi, J. Coutant, and R. Dautray, Las. Part. Beam **4**, 531 (1986).